Effect of Molecular Structure on the Linear Viscoelastic Behavior of Polyethylene

Paula M. Wood-Adams* and John M. Dealy*

Department of Chemical Engineering, McGill University, 3610 University Street, Montreal, Quebec H3A 2B2, Canada

A. Willem deGroot

The Dow Chemical Company, 2301 Brazosport Blvd, Freeport, Texas 77541

O. David Redwine

The Dow Chemical Company, Midland, Michigan 48667

Received September 9, 1999

ABSTRACT: The effects of weight-average molecular weight (M_W) and short and long chain branching on the linear viscoelastic behavior of polyethylene (and ethylene−α-olefin copolymers) are described. Short chain branching had no effect up to a comonomer (butene) content of 21.2 wt %. The zero shear viscosity of the linear polyethylenes scaled in the expected manner with M_W. Using a high molecular weight, narrow molecular weight distribution (MWD), linear polyethylene, an estimate of the plateau modulus and molecular weight between entanglements (M_e) was obtained. A solution property based technique for quantifying levels of long chain branching well below 1 LCB/10^4C in polyethylene is presented. Also, the applicability of ^{13}C NMR for measuring such LCB levels is demonstrated. For metallocene polyethylene, long chain branching (LCB) increased the zero shear viscosity as compared to that of a linear material of the same molecular weight. LCB also broadened the relaxation spectrum by adding a long time relaxation mode that was not present for the linear polyethylene with the same MWD.

Introduction

The systematic study of the relationships between molecular structure and the rheological behavior of polyolefins has been seriously limited in the past by the lack of samples with controlled and simply described distributions of molecular weight and long chain branching (LCB). Polymers prepared using traditional catalyst systems have a fairly broad molecular weight distribution that is difficult to reproduce. While fractionation and the hydrogenation of polybutadiene can yield samples with narrow molecular weight distributions, the processes for their preparation are very tedious, and the amounts available for measurements are very small. This is a serious limitation, as many repeat measurements are required to establish the precision of experimental data.

While the preparation of monodisperse samples continues to be problematic, single site catalysts now make it possible to prepare samples in which the molecular weight distribution is relatively narrow and quite reproducible. In addition, a particular type of single-site catalyst, the constrained geometry catalyst (developed by The Dow Chemical Company), makes it possible to introduce low and well-controlled levels of long chain branching. We will use the term "metallocene polyethylene" (mPE) to describe materials made using the new catalysts. We have taken advantage of the availability of these materials to make a systematic study of the effects of molecular weight and long and short chain branching on the linear viscoelastic behavior of polyethylene.

We feel that, among rheological properties, it is the linear properties, for example the storage and loss moduli, that represent the richest source of information regarding molecular structure. This is partly because the techniques used for their measurement offer a combination of high precision, ease of use, and a broad range of time scales (frequencies). In addition, in shear, it appears that large, rapid deformations, i.e., those involving nonlinear viscoelasticity, yield data relatively deficient in detailed information regarding molecular structure. A possible exception is extensional flow, which is thought to be particularly sensitive to the presence of long chain branching. However, it is very difficult to obtain accurate data reflecting the response of a melt to extensional flows, and there is as yet no conclusive picture regarding the specific effects of LCB on this response.[1]

Since one of the primary objectives of this work was to describe the effect of long chain branching on the linear viscoelastic behavior of mPE, the quantification of LCB was of great importance. Therefore, LCB was quantified using three techniques. The rheology technique[1] is described in a companion paper. The second and third techniques, ^{13}C NMR and multidetector GPC measurements, are described in later sections.

Previous Work on Linear Monodisperse Polyethylenes

Raju et al.[2] studied the linear viscoelastic behavior of samples of high-density polyethylene (HDPE) that were prepared by fractionation of polydisperse materials. The samples studied by these authors had $M_W/M_N < 1.2$. Using these data, they were able to generate what has become the standard zero shear viscosity molecular weight relation for polyethylene at 190 °C (eq 1).

$$\eta_0\,(\text{Pa.s}) = 3.4 \times 10^{-15}(M_W)^{3.6} \qquad (1)$$

10.1021/ma991533z CCC: $19.00
Published on Web 09/06/2000

Raju et al.[2] also reported a value of 1.58 MPa for the plateau modulus, G_N^0, which they calculated by use of eq 2 for a high molecular weight polyethylene fraction (M_W = 265 000). Then using eq 3, they estimated the molecular weight between entanglements, M_e, to be 1850.

$$G_N^0 = \frac{2}{\pi}\int_{-\infty}^{\infty} G''(\omega)\, d \ln \omega \quad (2)$$

$$G_N^0 = \frac{\rho R T}{M_e} \quad (3)$$

Another model polymer used to study the relationship between molecular structure of polyethylene and its rheological behavior is hydrogenated polybutadiene (HPB). Polybutadiene can be synthesized by anionic polymerization, which allows very precise control over molecular structure. This material, which contains many unsaturated bonds, can then be hydrogenated to yield a polymer that is very similar to polyethylene. Hydrogenated polybutadiene can then be considered to be a nearly monodisperse analogue of polyethylene.

Raju et al.[3] studied the linear behavior of a series of polyethylene analogues prepared in this way and compared it with that of the fractionated samples studied by Raju et al.[2] They found that the relationship between η_0 and the molecular weight was the same for the two series of materials. However, the plateau modulus was estimated to be in the range 1.83−2.73 MPa at 190 °C for the various HPB samples, which places it well above the value reported for the fractionated sample. The entanglement molecular weight calculated from the "average" plateau modulus, 2.31 MPa, is 1250, which is currently the generally accepted value for HDPE.

LCB−Rheology Relations

One of the most challenging molecular structure−rheology relationships to study experimentally is the effect of LCB. The degree, length, and structure of the branching all affect the rheological behavior in various ways. Studies of the effect of LCB on rheological behavior are further complicated by variations in molecular weight distribution, since it is difficult to control independently these two characteristics by conventional polymer synthesis technology. Because of these complications and the fact that much work in this area has been based on comparing resins that are different in more than one aspect of molecular structure, we do not have a clear understanding of the effect of LCB on the rheological behavior of commercial polyethylene. However, there has been a significant amount of work done with model polymers such as stars or combs that have very narrow molecular weight distributions and uniform structures. According to Soares and Hamielec,[4] the branched metallocene polyethylenes that we studied can be considered to be mixtures of linear, T-shaped, and H-shaped molecules, with very small amounts of more highly branched molecules.

Many studies of star polymers have been reported. Graessley et al.[5] and Raju et al.[2] have observed viscosity enhancement, i.e., an increase in zero shear viscosity of a branched polymer over that of a linear polymer of equivalent molecular size for stars of polyisoprene and hydrogenated polybutadiene (HPB). Raju et al.[2] also demonstrated that the zero shear viscosity of star branched hydrogenated polybutadiene depends exponentially on arm molecular weight, and Carella et al.[6] and Fetters et al.[7] confirmed this finding. Graessley and Raju[8] reported that the amount of viscosity enhancement is independent of the number of arms for stars of HPB of the same total molecular weight.

According to Roovers,[9] the maximum in the loss modulus that occurs in the plateau zone for star polymers is a result of arm relaxation, and the inverse of the frequency at which this occurs is the characteristic time for this relaxation process. He reports that for stars having the same arm molecular weight the frequency at the maximum in the loss modulus is independent of the number of arms.

Jordan et al.[10] and Gell et al.[11] have examined the question of how long a branch must be before it is considered to be a long branch in terms of its impact on rheological behavior. Jordan et al.[10] studied a series of asymmetric three-arm stars of deuterated polybutadienes. These materials had two branches of equal length, considered to be the backbone, and a third branch varied in length from approximately 7% to 50% of the backbone length (i.e., a symmetric star). On the basis of diffusion measurements, Jordan et al.[10] concluded that materials with branches longer than $2M_e$ behaved as long chain branched polymers. For polyethylene, M_e is 1250, therefore branches would have to be on the order of 180 carbons in length to be considered a long branch in terms of its impact on rheological behavior.

Gell et al.[11] studied a similar series of asymmetric three-arm stars of poly(ethylene-*alt*-propylene), PEP. The length of the branch varied from approximately 1% of the backbone length to 50% of the backbone length for their materials. They found that the relaxation spectrum broadens quickly with increased branch length. The authors observed dynamic modulii curves that indicated separate relaxation modes for the branch and the backbone starting at $M_{branch} = 2.4M_e$. On the basis of this result and self-diffusion experiments, they concluded that branches with 2−3 entanglements are long enough to result in branched polymer rheological behavior. They also mention that this is a much lower entanglement number than is necessary for symmetric star polymers to exhibit branched polymer behavior, which indicates that branches can affect the rheological behavior earlier when they are much shorter than the backbone.

Roovers[12] studied the linear viscoelastic behavior of H-shaped polystyrenes. He found that, for the same molecular size, H-shaped polymers exhibit a higher degree of viscosity enhancement than three- and four-arm stars. The dynamic moduli of the H-shaped polymers are qualitatively similar to those of stars in that there is a general broadening of the relaxation behavior with the addition of long-time relaxation processes that are not present for linear materials.

Graessley and Raju[8] studied blends of linear and star branched HPB where both constituents had similar zero shear viscosities. Since the star branched materials exhibited viscosity enhancement, the molecular weights of the two components in the blend were not the same. The zero shear viscosities of the blends were not less than those of the pure components. The authors interpreted this to mean that the viscosity enhancement does not depend on the interaction between two branched molecules but rather on the interaction of a branched chain with other entangled chains. Struglinski et al.[13]

Table 1. Linear Homopolymers

resin	M_W DRI	M_W LALLS	M_W/M_N DRI
HDL2	39 557	38 000	1.90
HDL3	113 386	112 000	2.02
HDL4	327 000	329 000	2.08

Table 2. Linear Butene Copolymers

resin	M_W DRI	M_W LALLS	M_W/M_N DRI	wt % butene
HDL1	94 000	93 000	2.08	1.4
LDL1	110 000	109 000	2.30	11.4
LDL2	98 000	97 000	2.08	14.83
LDL3	121 000	120 000	2.12	21.2

reported similar results for blends of linear and star polybutadienes. Their loss and storage modulus data for the blends showed a smooth transition with increasing volume fraction of branched material from the behavior of the pure linear material to the behavior of the pure branched material. The blends exhibited both the slower relaxation behavior of the branched material and the sharp high-frequency maximum in the loss modulus of the linear constituent.

While work with model branched polymers has enhanced our understanding of the effects of LCB, the structures of these materials are quite different from those of industrial materials. Thus, studies involving more realistic systems are of interest although more difficult to interpret. Kasehagen et al.[14] have reported the rheological behavior of randomly branched polybutadienes produced by adding increasing numbers of branches to two essentially monodisperse polybutadiene precursors. The authors reported the expected broadening of the relaxation spectrum with increased LCB. An additional relaxation regime between the plateau and the terminal region was present for the branched materials but not for the linear precursors. They also found that the zero shear viscosity and steady-state compliance increased with LCB.

Materials

To reach meaningful conclusions about the effect of molecular structure on rheological behavior, it is necessary to make a judicious choice of the materials to be studied. In particular, it is necessary to work with groups of materials that differ in only one molecular characteristic. As mentioned earlier, the new catalyst technologies make it possible to synthesize such groups of materials.

The linear homopolymers listed in Table 2, HDL2−4, were produced in a batch polymerization process using a "constrained geometry" catalyst of the type described by Stevens.[15,16] The long chain branched polymers listed in Table 1, LDB1−3 and HDB1−4, were synthesized using the same catalyst in the solvent phase in a continuous, stirred-tank reactor, as described by Lai et al.[17] Soares and Hamielec[18] have explained why this arrangement is optimal for LCB formation. Branching occurs by the insertion of vinyl-terminated polymer chains to active centers during polymerization. These "macromonomers" are formed primarily by β-hydride elimination. Soares and Hamielec have developed kinetic models for this process for the synthesis of both homopolymers[18] and copolymers,[19] and their models indicate that nearly all of the branched molecules in the branched polymers used in the present study contain a single branch.

Sample HDL1 was polymerized in a slurry process on a supported constrained geometry catalyst system. Samples LDL1−3 (Table 3) are commercial Exact polymers made by Exxon. Samples LLDPE1 and LLDPE2 (Table 4) are commercial products of The Dow Chemical Company and were produced in a continuous solution process with a heterogeneous Ziegler−Natta catalyst.

These materials comprise several sets that allowed us to study the effect of MW, SCB, and LCB on rheological behavior. The linear mPE homopolymers with molecular weights in the range 38 000 to 329 000 (Table 1) were used to examine the effect of weight-average molecular weight. To study the effects of short chain branching, the four linear ethylene−butene copolymers (Table 2) were used. Two series of long chain branched metallocene polyethylenes were also studied (Table 3). Within each of these series the materials have approximately the same molecular weight distribution, and comonomer content in the case of the low-density resins, but different levels of long chain branching. These materials allowed us to study the effects of LCB on the rheological behavior of these materials. Finally, for comparison purposes the two traditional linear low-density polyethylene resins were included (Table 4).

Experimental Section

Molecular weight distributions were determined by high-temperature gel permeation chromatography (GPC) using a differential refractive index (DRI) detector. The system consisted of a Waters 150C GPC with three Polymer Laboratories Mixed-B 10 μm columns. Calibration was performed with narrow MWD polystyrene standards, and universal calibration was applied using the following Mark−Houwink coefficients:

$$\text{for polystyrene:} \quad [\eta] = 1.26 \times 10^{-4} M^{0.702}$$

$$\text{for polyethylene:} \quad [\eta] = 3.8 \times 10^{-4} M^{0.73}$$

Additional experimental details of the GPC method are given in Table 5.

Absolute molecular weights were determined for some materials on a Polymer Laboratories PL210 high-temperature GPC equipped with a Viscotek model 210R viscometer and a Precision Detectors PD2000 light scattering instrument. The system was calibrated using a standard material (NBS 1475) with a weight-average molecular weight of 52 000 and an intrinsic viscosity of 1.01 dL/g. Detector offsets were determined using the systematic approach of Mourey and Balke.[20] Data from these measurements were also used to quantify long chain branching as described in the next section. All long chain branching determinations were made on the average of from 6 to 12 injections. Table 6 gives the experimental details for this system.

The molecular weight distributions for the materials are shown in Figures 1−4. In Figure 4 the molecular weight distribution functions are plotted against the reduced molecular weight ($m \equiv M/M_W$). The data are plotted in this way to allow the comparison of the shapes of the distributions.

LCB measurements for the homopolymers were performed using ^{13}C NMR. The 150 MHz spectra were obtained using a Oxford 14.1 T magnet. A GE-Omega console was used for earlier experiments, which was later replaced by a Varian Inova console. Consistency between the two instruments was verified. Samples were prepared by dissolution of less than 1 g of polymer in 3 mL of a solvent composed of $^2/_3$ trichlorobenzene and $^1/_3$ tetrachloroethane-d_2 by volume. The resulting mixture also contained 0.05 M chromium(III) acetylacetonate as a nuclear spin relaxation agent. Each mixture was degassed to remove oxygen and then heated to 150 °C while agitating in a vortex mixer to dissolve the polymer. Degassing was performed either by repeated freeze−thaw cycles under vacuum or by passing argon through the sample. To further prevent oxidation of the polymer, the bore of the magnet was purged with nitrogen during the NMR measurements.

Table 3. Long Chain Branched MPEs

resin	comonomer	density	M_W DRI[a]	M_W LALLS	M_W/M_N DRI	LCB/10^4C ^{13}C NMR	LCB/10^4C rheology	LCB/10^4C GPC
LDB1	octene	0.908	102 000		2.21		0.12	0.1
LDB2	octene	0.908	84 000		2.21		0.41	0.4
LDB3	octene	0.908	83 000		2.32		0.53	0.6
HDB1	none	0.9592	78 000	77 000	1.98	0.26	0.27	0.3
HDB2	none	0.9583	80 000	82 000	1.93	0.37	0.41	0.3
HDB3	none	0.9575	82 000	86 000	1.99	0.42	0.46	0.4
HDB4	none	0.9565	84 000	96 000	2.14	0.80	0.76	0.8

[a] DRI = differential refractive index detector.

Table 4. Linear Low-Density Polyethylenes

resin	comonomer	density (g/cm^3)	M_W DRI	M_W/M_N DRI
LLDPE1	octene	0.91	158 000	4.54
LLDPE2	octene	0.91	145 500	3.50

Table 5. Gel Permeation Chromatography Experimental Conditions

columns	3 Polymer Laboratories 30 cm, 10 μm mixed bed columns, PL mixed B
guard column	1, 5 cm, 50A
solvent	1,2,4-trichlorobenzene
stabilizer	butylated hydroxytoluene (BHT)
stabilizer concn	180 ppm
flow rate	1.0 mL/min
injection vol	100 μL
type of detector	differential refractive index (DRI) detector
detector sensitivity	64
detector scale factor	4
temp of columns	145 °C
temp of injector	145 °C
temp of pump	55 °C
typical sample concn	0.1 g/50 mL

Table 6. Polymer Laboratories PL210 Triple-Detector GPC Experimental Conditions

columns	3 Polymer Laboratories 30 cm, 10 μm mixed bed columns, PL mixed B
guard column	1, 5 cm, 50A
solvent	1,2,4-trichlorobenzene
stabilizer	butylated hydroxytoluene (BHT)
stabilizer concn	180 ppm
flow rate	1.0 mL/min
injection vol	100 μL
type of detector	differential refractive index (DRI) detector, PD2000 LS detector, Viscotek model 210R viscometer
dn/dc	0.104 mL/g
temp of columns	145 °C
temp of injector	145 °C
typical sample concn	0.1 g/50 mL

Data were collected using one of three probes: a standard GE 10 mm broad-band probe tuned to 150 MHz (ASTM S/N 600:1, 3500 Hz decoupler field, PW90 25 μs), a Nalorac Z-Spec 10 mm broad-band probe built for the GE system (ASTM S/N 800:1, 4000 Hz decoupler field, PW90 25 μs), or a Nalorac Z-Spec 10 mm broad-band probe built for the Varian system (ASTM S/N 1050:1, 4250 Hz decoupler field, PW90 14 μs). A relaxation delay of 0.5−1.0 s was used between 90° radio-frequency pulses to collect between 50 000 and 2 000 000 transients.

In ^{13}C NMR it is necessary to decouple proton spin from carbon spin, thus generating a spectrum consisting of only carbon singlets. With the Nalorac probes continuous wave (CW) decoupling was used. This prevents the cycling sidebands, which occur when using a modulated decoupling scheme. As described in a later section, the presence of cycling sidebands in some of the earlier measurements prevented the resolution of C4 branches from longer branches. With the GE probe the CW decoupling field was not adequate, and a WALTZ[21] decoupling scheme was used. When WALTZ decoupling was required, the decoupler position, power level, and modulation rate were adjusted to prevent sidebands in the region of the methine carbon (ca. 38.2 ppm).

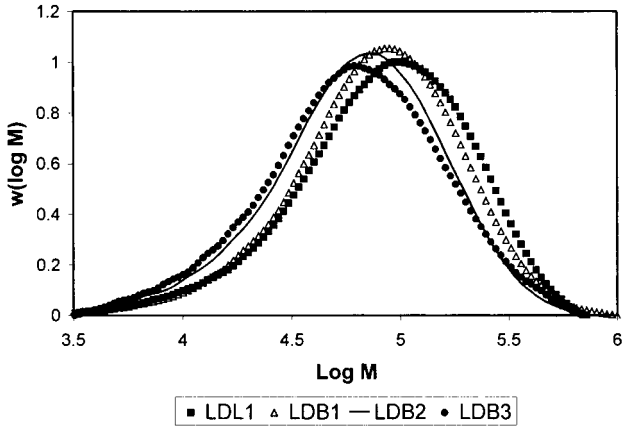

Figure 1. Comparison the MWDs of the butene−ethylene copolymers.

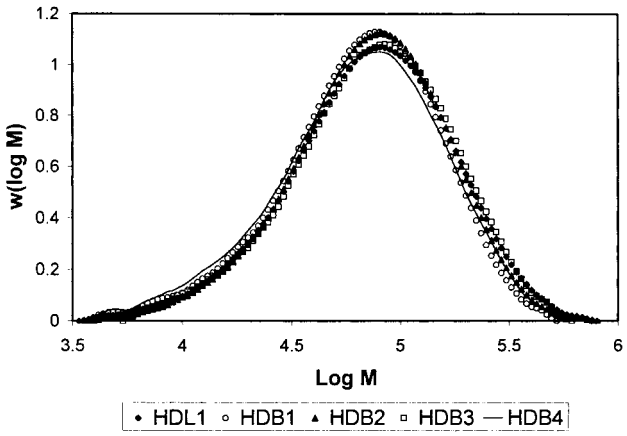

Figure 2. Comparison the MWDs of the high-density long chain branched materials.

A localized seventh-order polynomial baseline correction was used to correct the spectra in the aliphatic region of the spectrum. A second localized linear baseline correction was used to correct the methine peak and the peaks for the α and β carbons. The natural line width for the methine resonance was typically 4−6 Hz, which, when apodized with an exponential function of the same width, gives a resulting line width of 8−12 Hz.

LCB estimates for all polymers were also obtained using the technique described by Wood-Adams and Dealy.[1] This technique involves using GPC data in conjunction with linear viscoelastic data to estimate the degree of LCB. All of the linear materials in Tables 1 and 2 were also subjected to this technique, yielding results that confirmed the absence of long branches.

The dynamic LVE data were collected by use of a Rheometrics dynamic analyzer II (RDA II) in parallel plate (25 mm diameter) configuration with a gap of 1 mm. All experiments

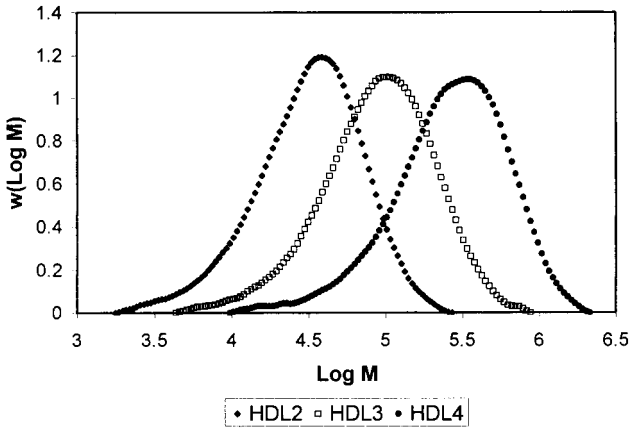

Figure 3. Comparison the MWDs of the linear homopolymers.

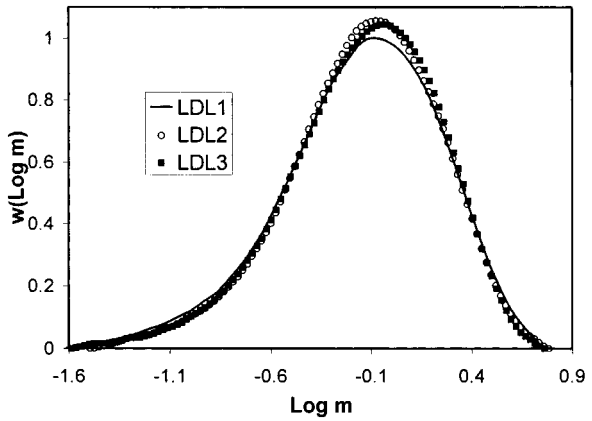

Figure 4. Comparison the MWDs of the linear butene–ethylene copolymers.

were performed under a nitrogen atmosphere, and resin stability under testing conditions was verified. This instrument has a spring torque transducer with a range of 2–2000 g·cm, and torques above 5 g·cm were assumed to be reliable [1 g·cm = 9.8 × 10^{-5} N·m]. Prior to performing frequency sweeps, strain sweeps were performed to establish the linear region at each frequency. For the frequency sweeps the variable strain technique was used, which entails using the maximum strain still within the linear region for each frequency. Measurements were performed at 150 °C. All data sets reported here are the average of several repeat measurements performed with different samples.

LCB Characterization Using Triple-Detector GPC

Multidetector GPC is a very powerful method for characterizing long chain branching in polymers[22] although there has been some controversy about its utility in the case of low levels of LCB.[23] In this study we used a triple-detector GPC setup as described in the Experimental Section to demonstrate that such measurements can be used to quantify LCB at levels well below 1 LCB/10^4C.

Triple-detector GPC allows the simultaneous and independent determination of intrinsic viscosity and molecular weight for each fraction of the polymer. Double-logarithmic plots of intrinsic viscosity versus molecular weight can then be generated that cover the entire distribution of molecular weights for any given sample. Such plots, generally referred to as Mark–Houwink plots, can be used to qualitatively describe the molecular structure. A quantitative description of the molecular structure can be made by applying the Mark–Houwink and Zimm–Stockmayer[24] relations to these data.

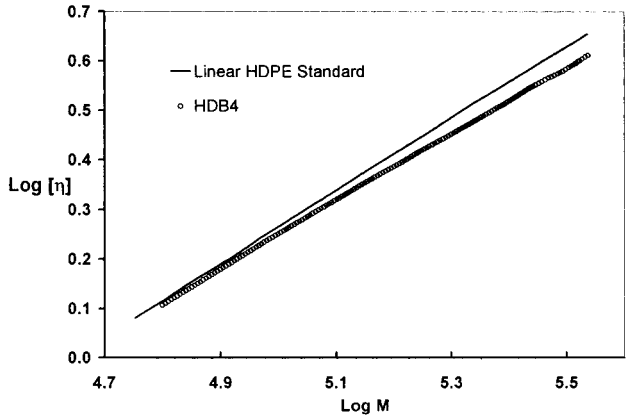

Figure 5. Effect of LCB on the Mark–Houwink plot.

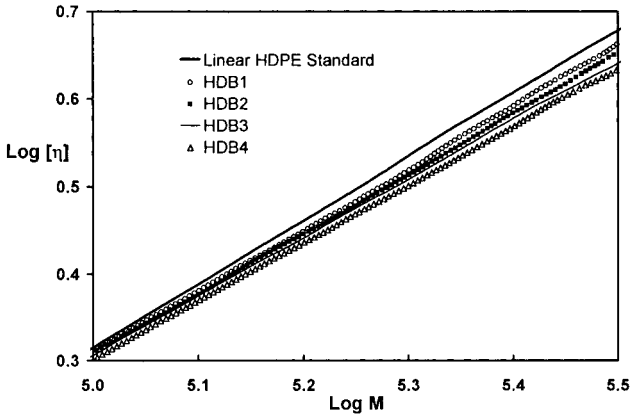

Figure 6. Mark–Houwink plot for HD series of materials.

Figure 5 shows a Mark–Houwink plot comparing a linear polyethylene homopolymer standard to sample HDB4. As expected from the Mark–Houwink relation, the data for the linear HDPE follow a straight line. The slope and intercept of this line give the Mark–Houwink parameters (eq 4).

$$[\eta] = 3.8 \times 10^{-4} M_W^{0.73} \quad (4)$$

Here $[\eta]$ is the intrinsic viscosity in dL/g, and M_W is the molecular weight of the polymer. These values agree very well with values reported previously in the literature for polyethylene.[25] The data for the long chain branched sample exhibit the typical shape of a randomly branched polymer.[24] They intersect the data for the linear sample in the low molecular weight region and show the largest deviation in the high molecular weight region of the distribution. Figure 6 compares the results for all of the HD series of materials. Figure 7 shows the results for samples LDB1 through LDB3. In this case, there is a shift in LD samples from the linear HDPE sample due to the presence of octene in the LD samples. In fact, it can be seen that qualitatively the high levels of short chain branches have more of an effect on the solution properties than the long chain branches, since the shift from the linear HDPE is so large. The short chain branches, however, do not affect the slope of the curve while the long chain branches do. It is this important difference that allows us to make use of the intrinsic viscosity for quantifying LCB. The effect of SCB on the Mark–Houwink plot of a linear polyethylene is shown in Figure 8.

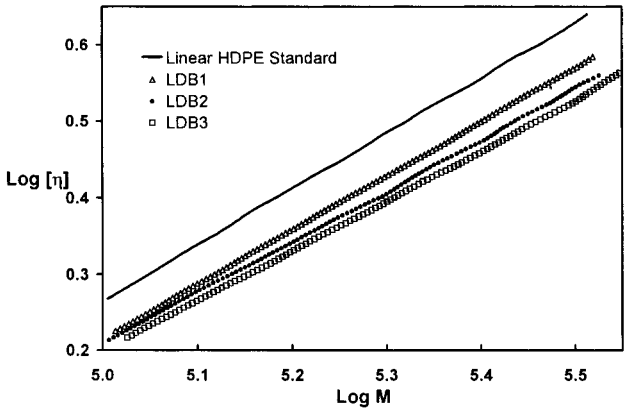

Figure 7. Mark−Houwink plot for LD series of materials.

Long chain branching calculations were performed for each fraction of the sample using eqs 5−7. The Zimm−Stockmayer equation (eq 5) relates the average number of branch units per molecule (m) and g, the branching factor, which is defined in eq 6.

$$\langle g_3(m)\rangle_{Av} = [(1 + m/7)^{1/2} + 4m/9\pi]^{1/2} \quad (5)$$

$$g \equiv \frac{\langle S^2\rangle_B}{\langle S^2\rangle_L} \quad (6)$$

In eq 6 S^2 is the mean-squared radius of gyration. In the triple-detector GPC experiment the intrinsic viscosity is measured rather than the radius of gyration; therefore, eq 7 is used to determine the value of g.

$$g^{\epsilon} = g' \equiv \frac{[\eta]_B}{[\eta]_L} \quad (7)$$

In this equation ϵ is a parameter that depends on the type of long chain branching and the solvent quality.[26] We have determined experimentally that a value of 0.5 is appropriate for these polymers.

For each fraction, the average number of branched points per molecule is converted into the average number of branches per 10^4C using eq 8. Finally, the overall average LCB/10^4C is calculated using eq 9.

$$\left.\frac{LCB}{10^4C}\right|_{M_i} = \frac{m(14 \times 10^4)}{M_i} \quad (8)$$

$$\frac{LCB}{10^4C} = \sum w_i \left.\frac{LCB}{10^4C}\right|_{M_i} \quad (9)$$

Table 3 gives the results of the long chain branch determinations by triple-detector GPC. As can be seen, the solution property results agree reasonably well with the results from ^{13}C NMR for the HDB series of samples. This is true for the LDB series of samples and the rheological quantification results as well.

One clear conclusion from these results is the high sensitivity of this method to low levels of long chain branching in these materials. This is contrary to some previous reports.[23] The best explanation of this finding is that the branched samples studied here are randomly branched. This means there are very long branches on the highest molecular weight molecules. Since the light scattering detector and the viscometer are the most sensitive to high molecular weight polymer, there is plenty of detector signals and, thus, very high quality data from this part of the molecular weight distribution. The data quality is improved further by making multiple runs of both the linear and the branched polymers.

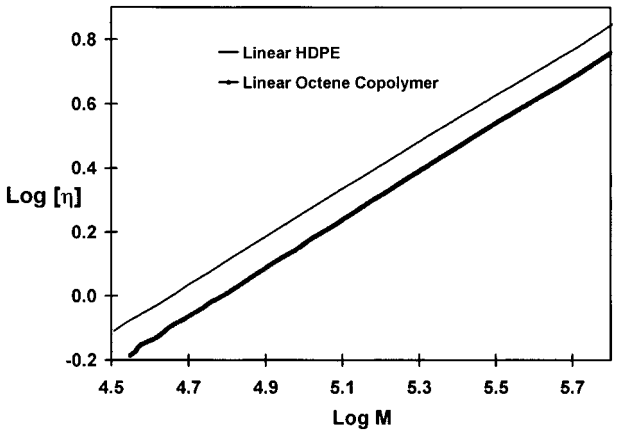

Figure 8. Effect of short chain branching on the Mark−Houwink plot.

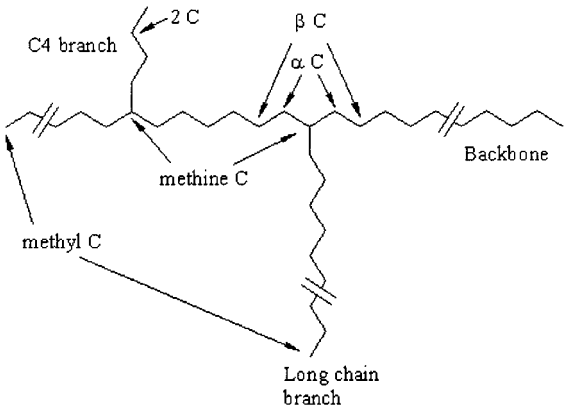

Figure 9. Microstructure of long chain branched mPE.

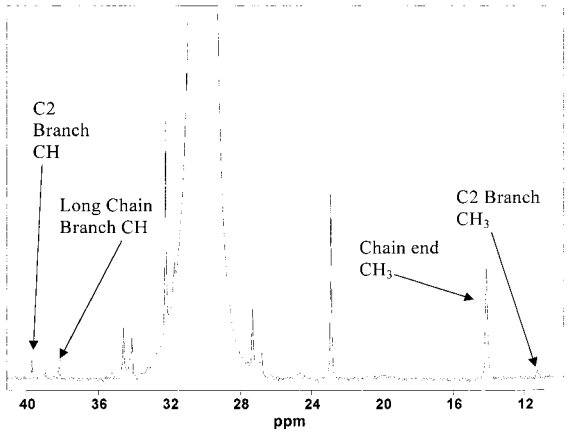

Figure 10. ^{13}C NMR spectrum for HDB1.

LCB Characterization Using ^{13}C Nuclear Magnetic Resonance

Long chain branch levels were calculated from ^{13}C NMR data using the methods described by Randall.[27] Figure 9 illustrates the microstructure of a long chain branched mPE and the nomenclature used to describe the various carbons. The spectrum for HDB1 is presented in Figure 10. The largest resonance, which occurs at 30.0 ppm, is due to the methylene carbons on the backbones and on the long chain branches. The reso-

Table 7. ^{13}C NMR Precision Study

resin	sample 1 (LCB/10^4*C*)	sample 2 (LCB/10^4*C*)	sample 3 (LCB/10^4*C*)
HDB1	0.029	0.026	0.023
HDB4	0.77	0.75	0.88

nances for the α, β, and γ carbons occur at 34.6, 27.2, and 32.2 ppm, respectively. The LCB was quantified by comparing the LCB methine resonance (38.2 ppm) to the methylene resonance.

The methine resonance was the preferred resonance due to the lack of any interfering resonances for these samples. In some cases these materials have branches that are four carbons in length (C4 branches). When such branches are present, it is necessary to correct the LCB methine intensity. We used the integrated intensity of carbon-2 of the C4 branch for this correction.

Triplicate measurements were performed on two of the samples to study the precision of the NMR analysis (Table 7). A result previously reported for HDB4[28] was discarded on the basis of this study. This original measurement, made using WALTZ decoupling, shows a modulation sideband in the region of carbon-2 of the C4 branch, making it impossible to correct the data for any C4 branches. Data produced recently for HDB4 using CW decoupling shows that some C4 branches are present in this polymer. We have found that the precision of the ^{13}C analysis of long chain branching is 10−20% relative at the 95% confidence level. This level of precision is expected for data that have a signal-to-noise (root-mean-square) ratio of approximately 10 or greater. Higher signal-to-noise ratios will give better precision but at the expense of extended data acquisition times.

Accuracy of the NMR experiment is governed primarily by the relative saturation of the peaks used to quantify branching and the main methylene resonance, which dominates the overall signal intensity. Traditionally, when selecting experimental conditions for quantitative NMR measurements, one aims for the highest possible accuracy. This results in very long delays between radio-frequency pulses. The key to success in quantifying these relatively low levels of LCB is to aim for a slightly reduced accuracy in the range 95−98%. Progressive saturation studies using ethylene octene copolymers as models indicate that the methine carbons and the main methylene carbons give a constant intensity ratio for sampling delays of 0.5 s or longer. With a sampling delay of 0.5−1 s the inaccuracy due to differential saturation is less than 5%. Further increases in sampling delay to achieve an accuracy closer to 100% result in analysis times up to 10 times longer. For lower levels of LCB shorter sampling delays are used (0.5 s), and more transients are collected.

On the basis of the results presented in this section, we conclude that ^{13}C NMR is an excellent method for measuring the low levels of LCB present in these polymers. The excellent agreement between the triple-detector results presented in the previous section, and the ^{13}C NMR results further support this conclusion.

Effect of Short Chain Branching

It is often assumed that short chain branching (SCB) has little or no effect on the rheological behavior of polyethylenes. Three of the linear mPEs included in this work, LDL1, LDL2, and LDL3, all of which are butene copolymers, provided an opportunity to test this assumption. These three resins have very similar polydispersities but varying levels of SCB.

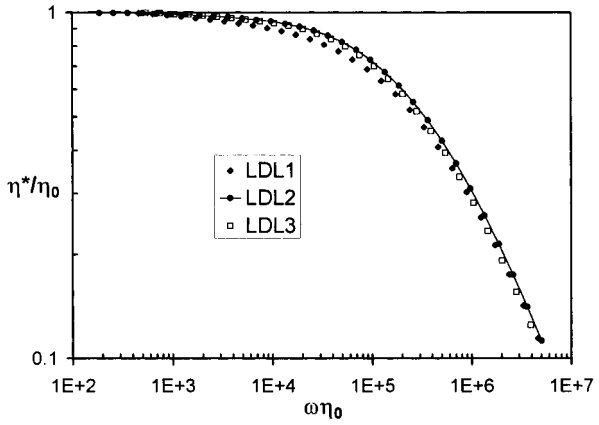

Figure 11. Effect of SCB on complex viscosity. The units of η_0 and ω are Pa·s and rad/s.

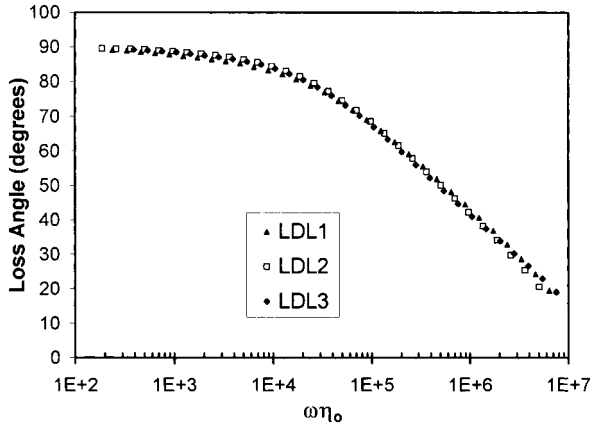

Figure 12. Effect of SCB on loss angle. The units of η_0 and ω are Pa·s and rad/s.

To remove the effects of M_W on the complex viscosity, the data are shifted on both axes by use of the zero shear viscosity (Figure 11). There are small differences between the three curves, but it is believed that these result from small differences in MWD (Figure 4). Another sensitive indicator of differences between materials is the loss angle.[29] For the three short chain branched materials, plots of loss angle versus shifted frequency are very similar (Figure 12). In a related study it was found that short chain branching has no effect on the ability of the viscosity−MWD to predict the GPC MWD.[1] On the basis of these observations, we conclude that for these three materials there is no significant effect of SCB on the LVE behavior. There is some controversy about this particular issue as has been reported that SCB affects the plateau modulus.[30] There was no such effect apparent in these data.

Effect of Weight-Average Molecular Weight

The seven linear mPEs described in Tables 1 and 2 were used to study the effect of weight-average molecular weight (M_W) on the LVE behavior. This ranged from 38 000 for HDL2 to 329 000 for HDL4. All of the materials included in this study had polydispersities of approximately 2, and we have already noted that SCB has no significant effect on the viscosity curve. Therefore, the differences in the complex viscosity curves (Figure 13) are primarily due to molecular weight variation. An increase in molecular weight causes an

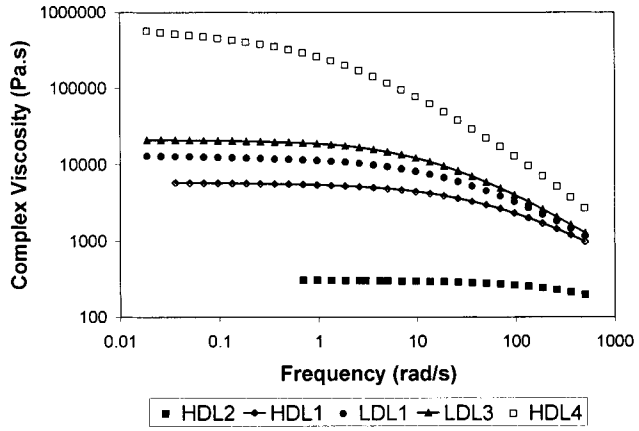

Figure 13. Effect of M_W on complex viscosity of linear mPEs (150 °C).

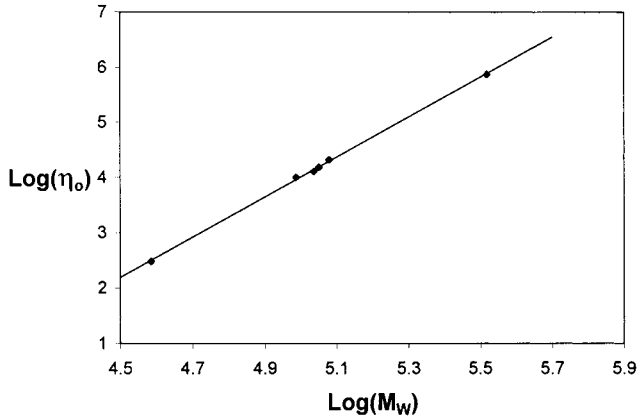

Figure 14. Relationship between zero shear viscosity (Pa·s) and M_W for linear mPEs (150 °C). The points are experimental data, and the line represents the best fit of eq 1.

increase in the zero shear viscosity and a decrease in the frequency at which shear thinning begins.

It was impossible to determine experimentally the zero shear viscosity for any of the materials except the one with the lowest molecular weight. Therefore, an estimate of η_0 was obtained using discrete relaxation spectra determined using IRIS software.[31] These data are plotted against weight-average molecular weight (LALLS) in Figure 14 using a double-logarithmic plot. In accord with eq 1, the data fall on a straight line. The parameters that result from fitting these data to eq 1 are $K = 6.8 \times 10^{-15}$ and $\alpha = 3.6$. These values are in good agreement with those reported by Raju et al.[2] for polyethylene at 190 °C ($K = 3.4 \times 10^{-15}$, $\alpha = 3.6$).

The effect of M_W on the loss angle is shown in Figure 15. The approach of the loss angle to 90° indicates that the data are approaching the terminal zone although it has not yet been reached. Increasing M_W decreases the frequency at which elasticity begins to play an important role. A M_W-independent plot of the loss angle can be generated by plotting the data against the product of the zero shear viscosity and frequency as in Figures 12 and 16.

The effect of M_W on the storage modulus is shown in Figure 17. Using loss modulus data for the highest M_W material (HDL4) after eliminating the high-frequency data, which were affected by instrument compliance, it was possible to estimate the plateau modulus by use of eq 2. To use eq 2, it was necessary to extrapolate the data at both low and high frequencies, as shown in Figure 18. The low-frequency end was extrapolated using the discrete spectrum, and the high-frequency end was extrapolated linearly using the last four accepted experimental points. Numerical integration yielded a value of 1.9 MPa for G_N^0 at 150 °C. This is plotted in Figure 17 for comparison with the storage modulus data.

Using eq 3, it was then possible to calculate a molecular weight between entanglements, M_e, which was determined to be 1460 g/mol. The values for M_e and G_N^0 can be compared with those reported by Raju et al.,[3] which were 2.3 MPa (190 °C) and 1250 g/mol, respectively. Our estimate of G_N^0 is slightly lower than theirs.

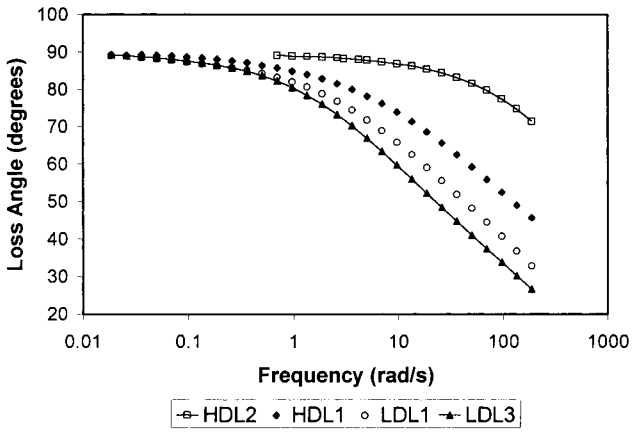

Figure 15. Effect of M_W on loss angle of linear mPEs (150 °C).

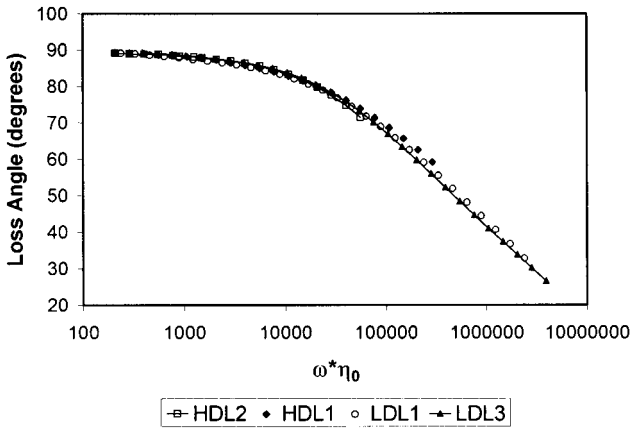

Figure 16. M_W-independent plot of loss angle (150 °C).

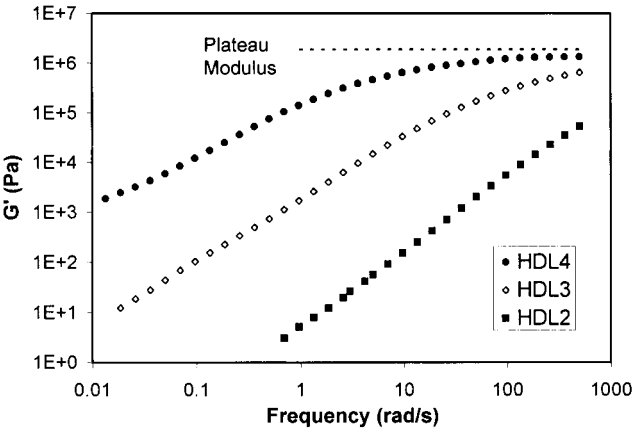

Figure 17. Effect of M_W on storage modulus. Plateau modulus estimated using loss modulus data as described in text.

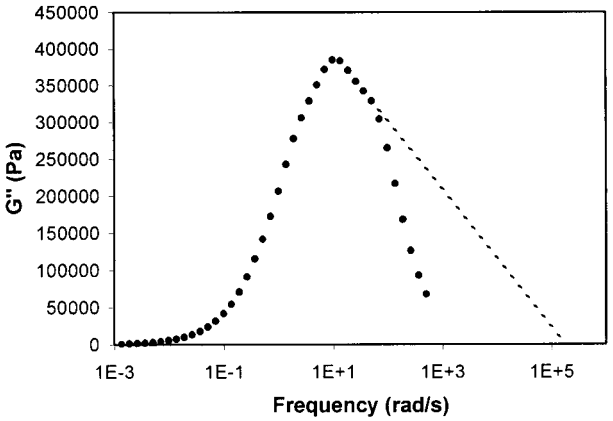

Figure 18. Extrapolation of loss modulus curve for HDL4 (150 °C).

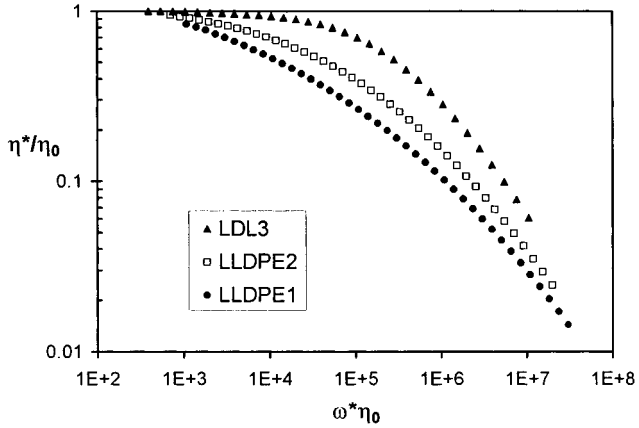

Figure 19. Effect of polydispersity on complex viscosity.

Effect of Breadth of MWD

The effect of broadening the molecular weight distribution on the linear behavior is shown in Figures 19 and 20. Figure 19 shows the effect of broadening the MWD on the complex viscosity, and we see the expected broadening of the transition zone between the Newtonian plateau and the high-frequency power law zone. Figure 20 shows this broadening effect in the loss angle.

As is shown in the following section, there are some similarities in the effects of polydispersity and long chain branching, but there are also important differences.

Effect of Long Chain Branching

It must be noted at this point that since the impact of LCB on rheological behavior is determined not only by number of branch points but also by branch length distribution and architecture. Therefore, the observations in this section are only directly applicable to materials polymerized under the conditions described earlier.

The complex viscosity curves for the high-density mPEs, HDB1−4 and HDL1, are compared in Figure 21. Long chain branching affects the complex viscosity in four ways: (1) the zero shear viscosity is increased for the same backbone molecular weight, (2) the amount of shear thinning is increased, (3) the transition zone between the zero shear viscosity and the power law zone is broadened, and (4) two points of inflection appear within the transition zone. These materials followed the Cox−Merz[32] rule as shown in Figure 21.

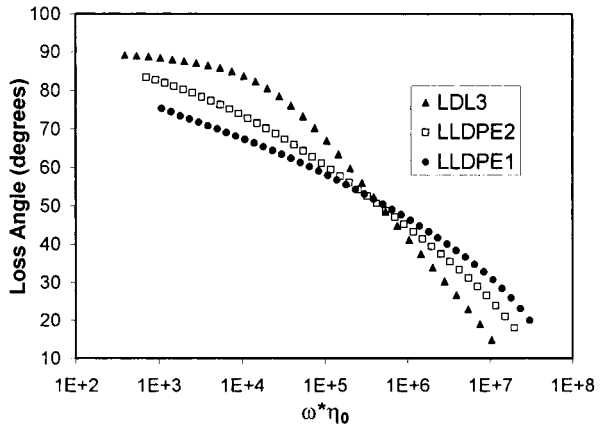

Figure 20. Effect of polydispersity on loss angle.

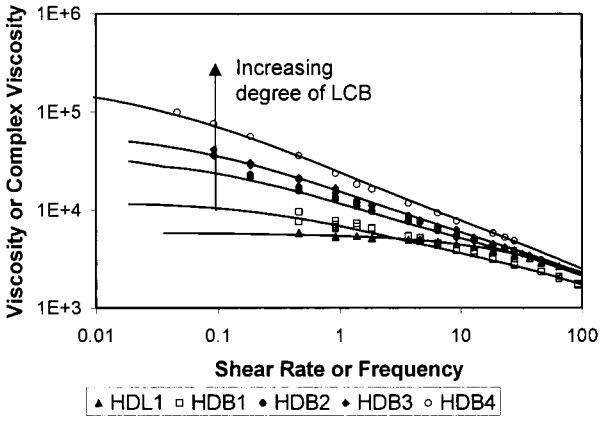

Figure 21. Viscosity and complex viscosity data for high-density mPEs. Solid lines are complex viscosity data, and symbols are viscosity data.

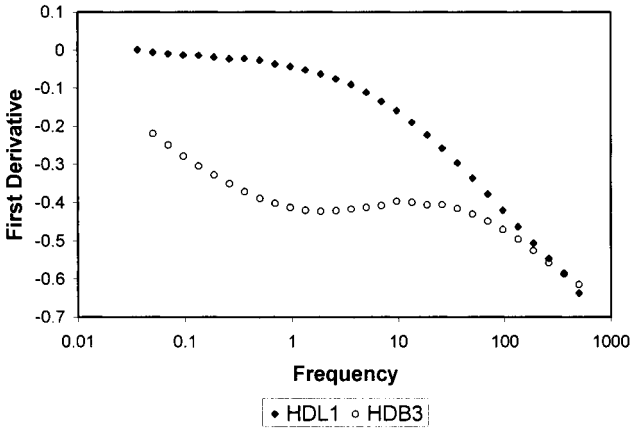

Figure 22. Comparison of first-derivative curves for HDB3 and HDL1.

These points of inflection in the complex viscosity can be seen more clearly by plotting the derivative of the logarithm of the complex viscosity (d ln η^*/d ln ω) as shown in Figure 22, where data for HDL1 (linear material) and HDB3 (0.42 LCB/10^4C) are compared. The inflection points show up as local minima and maxima in the curve for the branched material.

The effect of LCB on the zero shear viscosity is shown in Figure 23. In this figure the data are plotted in terms of the viscosity enhancement, which is the ratio of η_0 of the branched material to that of a linear material of the same molecular weight. As expected, increasing the degree of LCB increases the zero shear viscosity for low

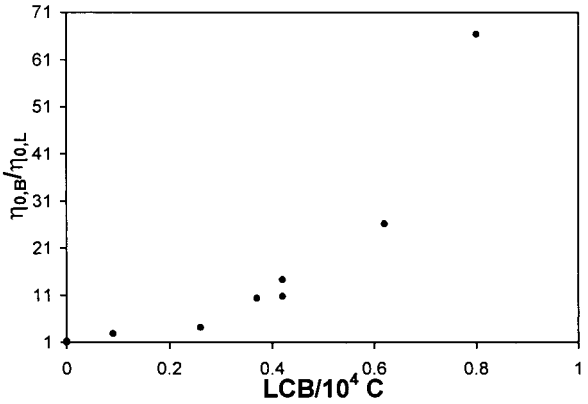

Figure 23. Effect of LCB on zero shear viscosity (150 °C): HD series and LD series.

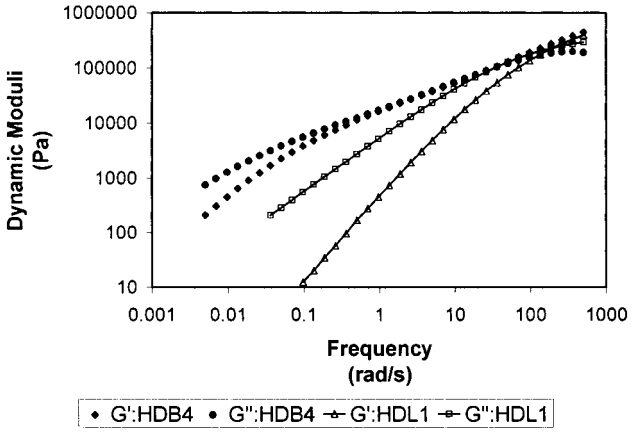

Figure 24. Comparison of dynamic moduli for HDB4 and HDL1.

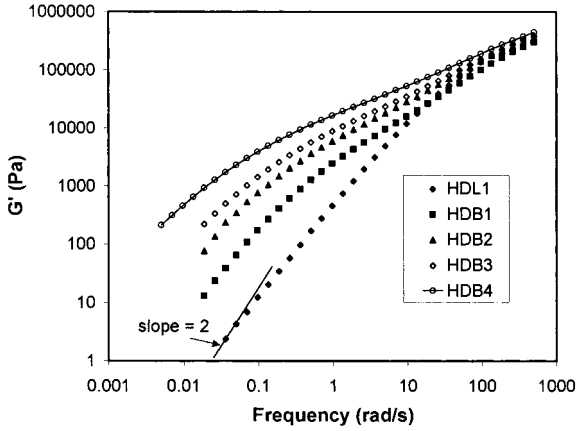

Figure 25. Effect of LCB on the storage modulus (HD series at 150 °C).

levels of LCB. Kim et al.,[33] Koopmans,[34] and Malmberg et al.[35] have also observed viscosity enhancement with long chain branched mPEs.

The effects of LCB can also be seen in other LVE properties such as the storage and loss moduli and the loss angle. In Figure 24 the dynamic moduli for HDB4 (branched) and HDL1 (linear) are plotted, and in Figure 25 the storage moduli of the HD materials are compared. Branching adds a mode of relaxation at low frequency that is not present in the linear material. Kasehagen et al.[14] showed that the storage modulus was a sensitive indicator of LCB for a series of randomly branched polybutadienes that were produced from a single linear monodisperse precursor. Branching in

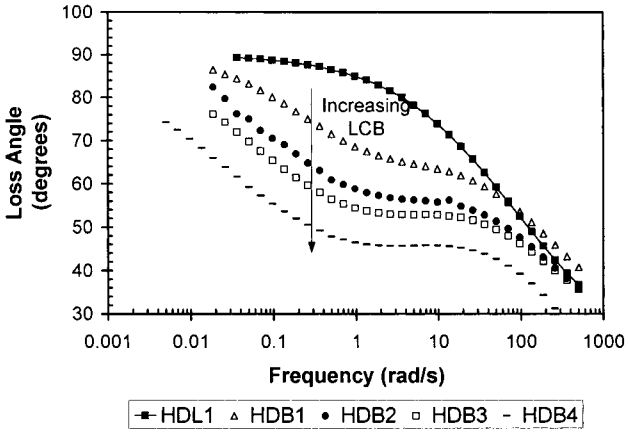

Figure 26. Effect of LCB on loss angle−high-density mPEs at 150 °C.

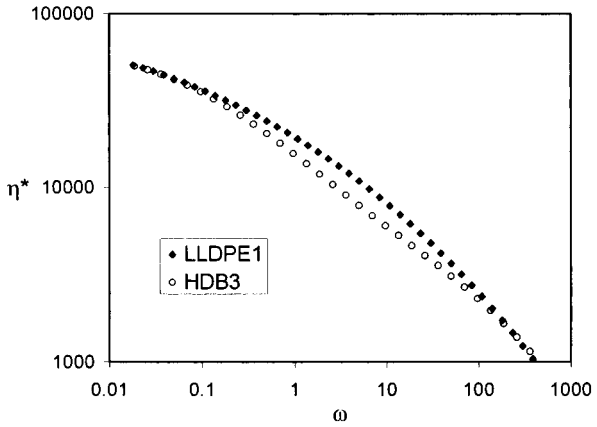

Figure 27. Comparison between the effect of polydispersity and LCB on the complex viscosity.

these materials also resulted in the appearance of a well-defined new relaxation regime. Hingmann and Marczinke[36] observed similar behavior with long chain branched polypropylene.

An even more sensitive indicator of the presence of LCB is the loss angle, which is shown in Figure 26. The loss angle curve for the linear material is what we would expect for a narrow MWD linear polymer, but the curves for the branched materials are quite different. We see a plateau in the loss angle, the magnitude and breadth of which depend on the degree of LCB. This observation is in accordance with results published by Koopmans,[34] who noted the same effect of LCB on loss angle when comparing an LDPE, an LLDPE, and two branched mPEs.

The effects of polydispersity and LCB on LVE behavior can be compared qualitatively by reference to data for LLDPE1 and HDB3 (Figure 27). These two materials have similar zero shear viscosities because of the difference in their molecular weights, and they also exhibit similar high-frequency behavior. But there is a significant difference between the curves in the intermediate frequency range.

It is perhaps surprising that these low levels of LCB have a marked effect on the LVE behavior, especially when one considers the behavior of highly branched LDPE. LDPE typically has a lower zero shear viscosity than a linear polyethylene with the same molecular weight and also usually exhibits a smaller decrease in complex viscosity with increasing frequency. However, LDPE and branched mPE have entirely different mo-

lecular structures. LDPE typically has a very broad MWD and many more than one branch points per molecule, while branched mPE has a narrow MWD and often less than one branch point per molecule. Therefore, it is not surprising that observations based on the behavior of LDPE cannot be extended to mPE. Also, because it is not possible to manufacture LDPEs with the same MWD but varying degrees of LCB, conclusions about the effect of level of LCB are difficult to make in the case of LDPE.

Conclusions

The zero shear viscosity was found to vary with the weight-average molecular weight to the 3.6 power for linear materials, confirming previously reported results. The degree of SCB, for butene copolymers, was shown to have no significant effect on the linear viscoelastic behavior up to a butene content of 21.2 wt %. The linear viscoelastic data are very sensitive to degree of LCB. The zero shear viscosity and breadth of relaxation spectrum increase with degree of LCB. Additionally, branched mPEs exhibit a plateau in their loss angle curve that is not present for linear polyethylenes. In terms of linear viscoelastic behavior, increasing the degree of long chain branching of mPEs has effects that are qualitatively similar to those of increasing the branch length in asymmetric star polymers. Triple-detector GPC and ^{13}C NMR were shown to be accurate techniques for quantifying LCB in mPEs.

Acknowledgment. Financial support for this work as well as the polymers used and all GPC and NMR data were provided by The Dow Chemical Company. Drs. Teresa Karjala and Steve Chum provided valuable advice.

Nomenclature

Greek Letters

δ = loss angle
η_o = zero shear viscosity
γ = strain
ρ = density
$\eta^*(\omega)$ = complex viscosity
ω = frequency

Roman Letters

$G(t)$ = linear shear stress relaxation modulus
M_e = critical mol wt for entanglement
$G'(\omega)$ = storage modulus
M_W = weight-average mol wt
$G''(\omega)$ = loss modulus
R = ideal gas constant
G_N^0 = plateau modulus
T = temp
$G^*(\omega)$ = complex modulus

References and Notes

(1) Wood-Adams, P. M.; Dealy, J. M. *Macromolecules* **2000**, *33*, 7481.
(2) Raju, V. R.; Smith, G. G.; Marin, G.; Knox, J. R.; Graessley, W. W. *J. Polym. Sci., Phys. Ed.* **1979**, *17*, 1183.
(3) Raju, V. R.; Rachapudy, H.; Graessley, W. W. *J. Polym. Sci., Phys. Ed.* **1979**, *17*, 1223.
(4) Soares, J.; Hamielec, A. In *Metallocene-Catalyzed Polymers: Materials, Properties, Processing and Markets*; Benedikt, G. M., Goodall, B., Eds.; Plastics Design Library: New York, 1998; pp 103−112.
(5) Graessley, W. W.; et al. *Macromolecules* **1976**, *9*, 127.
(6) Carella, J. M.; Gotro, J. T.; Graessley, W. W. *Macromolecules* **1986**, *19*, 659.
(7) Fetters, L. J.; Kiss, A. D.; Pearson, D. S.; Quack, G. F.; Vitus, F. J. *Macromolecules* **1993**, *26*, 647.
(8) Graessley, W. W.; Raju, V. R. *J. Polym. Sci., Polym. Symp.* **1984**, *71*, 77.
(9) Roovers, J. *Polymer* **1985**, *26*, 1091.
(10) Jordan, E. A.; Donald, A. M.; Fetters, L. J.; Klein, J. *ACS Polym. Prepr.* **1989**, *30*, 63.
(11) Gell, C. B.; Graessley, W. W.; Efstratiadis, V.; Pitsikalis, M.; Hadjichristidis, N. *J. Polym. Sci., Part B: Polym. Phys.* **1997**, *35*, 1943.
(12) Roovers, J. *Macromolecules* **1984**, *17*, 1196.
(13) Struglinski, M. J.; Graessley, W. W.; Fetters, L. J. *Macromolecules* **1988**, *21*, 783.
(14) Kasehagen, L. J.; Macosko, C. W.; Trowbridge, D.; Magnus, F. *J. Rheol.* **1996**, *40*, 689.
(15) Stevens, J. *Stud. Surf. Sci. Catal.* **1994**, *89*, 277.
(16) Stevens, J. *Stud. Surf. Sci. Catal.* **1996**, *101*, 11.
(17) Lai, S. Y.; Wilson, J. R.; Knight, J. R.; Stevens, G. W. U.S. Patent 5,272,236, 1993.
(18) Soares, J. B. P.; Hamielec, A. E. *Macromol. Theory Simul.* **1996**, *5*, 547.
(19) Soares, J. B. P.; Hamielec, A. E. *Macromol. Theory Simul.* **1997**, *6*, 591.
(20) Mourey, T. H.; Balke, S. T. *ACS Symp. Ser.* **1993**, *521*, 231.
(21) Shaka, A. J.; Keeler, J.; Freeman, R. *J. Magn. Reson.* **1983**, *53*, 313.
(22) Scholte, Th. G.; Meijerink, N. L. J. *Br. Polym. J.* **1977**, *6*, 133.
(23) Janzen, J.; Colby, R. *J. Mol. Struct.* **1999**, *485/486*, 569.
(24) Zimm, B. H.; Stockmayer, W. H. *J. Chem. Phys.* **1949**, *17*, 1301.
(25) Scholte, Th. G.; Meijerink, N. L. J.; Schoffeleers, H. M.; Brands, A. M. G. *J. Appl. Polym. Sci.* **1984**, *29*, 3763.
(26) Scholte, T. H. In *Developments in Polymer Characterization-4*; Dawkins, J. V., Ed.; Applied Science: New York, 1983; p 1.
(27) Randall, J. C. *J. Macromol. Sci., Rev. Macromol. Chem. Phys.* **1989**, *C29* (2&3), 201.
(28) Wood-Adams, P. M.; Dealy, J. M. *SPE ANTEC Technol. Pap.* **1999**, *45*, 1205.
(29) Booij, H. C.; Palmen, J. H. M. *Rheol. Acta* **1982**, *21*, 376.
(30) Fetters, L. J.; Lohse, D. J.; Richter, D.; Witten, T. A.; Zirkel, A. *Macromolecules* **1994**, *27*, 4639.
(31) Baumgaertel, M.; Winter, H. H. *Rheol. Acta* **1989**, *28*, 511.
(32) Cox, W. P.; Merz, E. H. *J. Polym. Sci.* **1958**, *28*, 619.
(33) Kim, Y. S.; Chung, C. I.; Lai, S. Y.; Hyun, K. S. *J. Appl. Polym. Sci.* **1996**, *59*, 125.
(34) Koopmans, R. J. *SPE ANTEC Technol. Pap.* **1997**, *43*, 1006.
(35) Malmberg, A.; Kokko, E.; Lehmus, P.; Löfgren, B.; Seppälä, J. *Macromolecules* **1998**, *31*, 8448.
(36) Hingmann, R.; Marczinke, B. L. *J. Rheol.* **1994**, *38*, 573.

MA991533Z